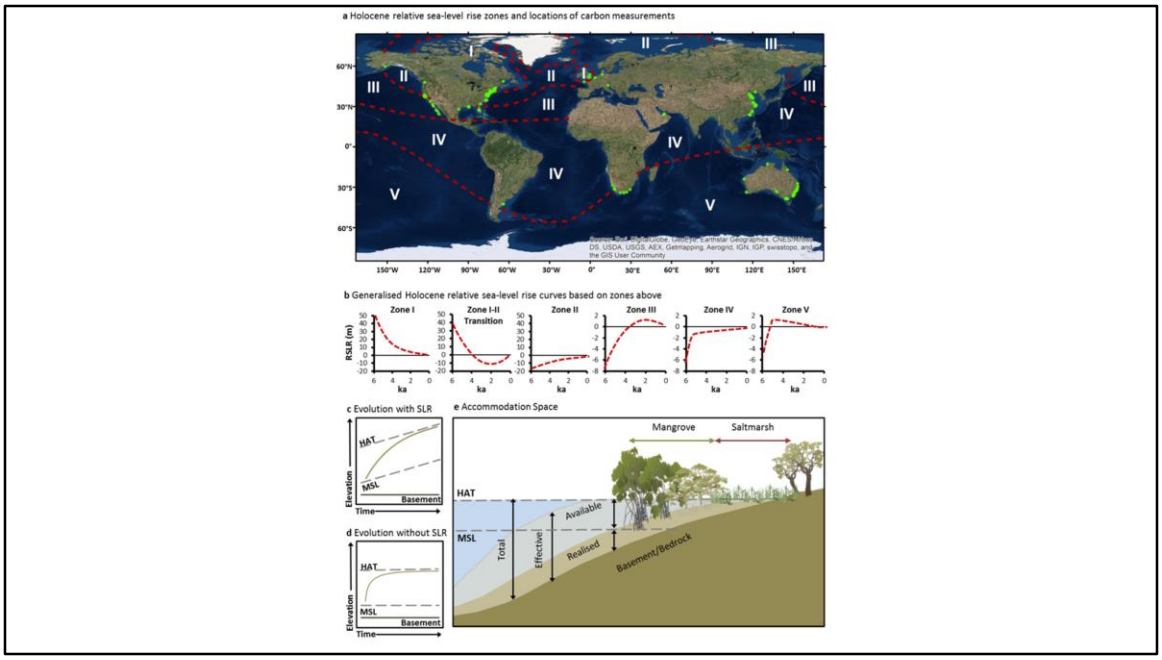

Fig. 1. Millennial-scale influence of relative sea level on wetland evolution and accommodation space. a) Generalised RSLR zones over the Holocene (from Clark et al.[9]), and sample data used in this study, shown as green spots (n=345 locations). b) Generalised relative sea-level history over past 6 millennia (from Clark et al.[9]). c) Wetland surface evolution within accommodation space, defined by highest astronomical tides (HAT) and mean sea level (MSL), which elevates as the sea rises. d) Wetland surface evolution within stable accommodation space, as occurred in southeastern Australia over late Holocene (from Allen[17]). e) Conceptualised wetland accommodation space, shown here in two-dimensions.

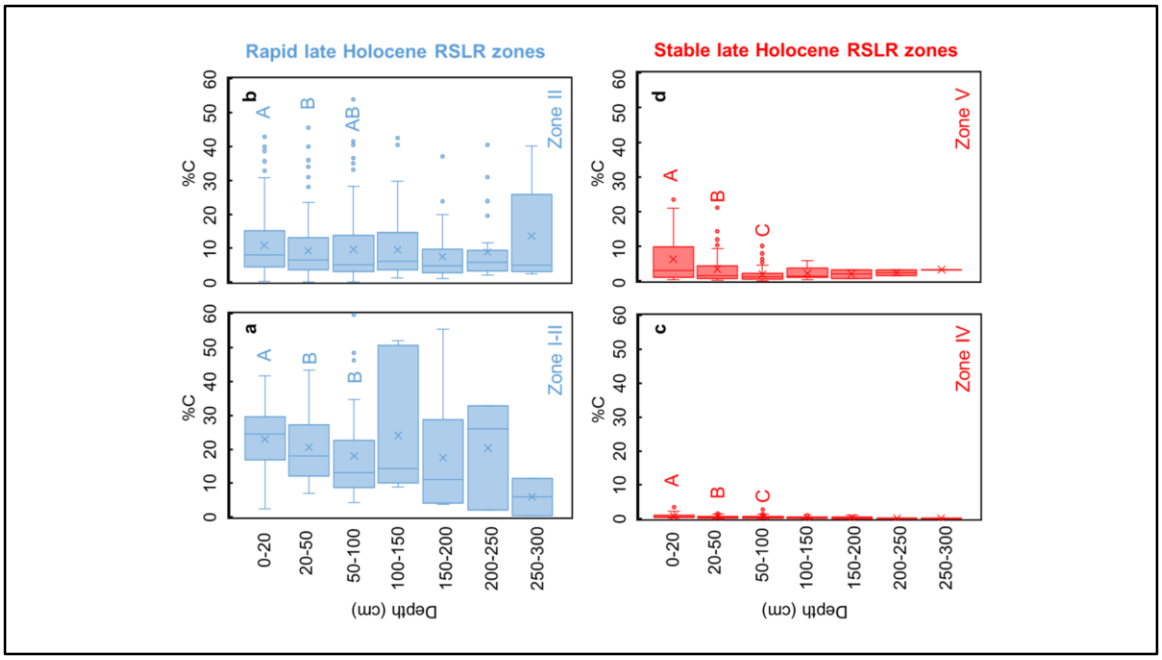

Figure 2: Influence of late-Holocene RSLR on C concentration. Tidal marshes located along coasts with rapid RSLR in the late Holocene contain higher %C than marshes along coasts with relatively stable sea level. %C over various depths from late Holocene RSLR a) zone I-II (rapid RSLR), b) zone II (rapid RSLR), c) zone IV (stable RSL) and d) zone V (stable RSL). Letters represent significant difference in %C among depths in the 0-100cm range within each RSLR zone. Boxplots for data poor RSLR zones (including I and III) are presented in Extended Data Fig. 1.

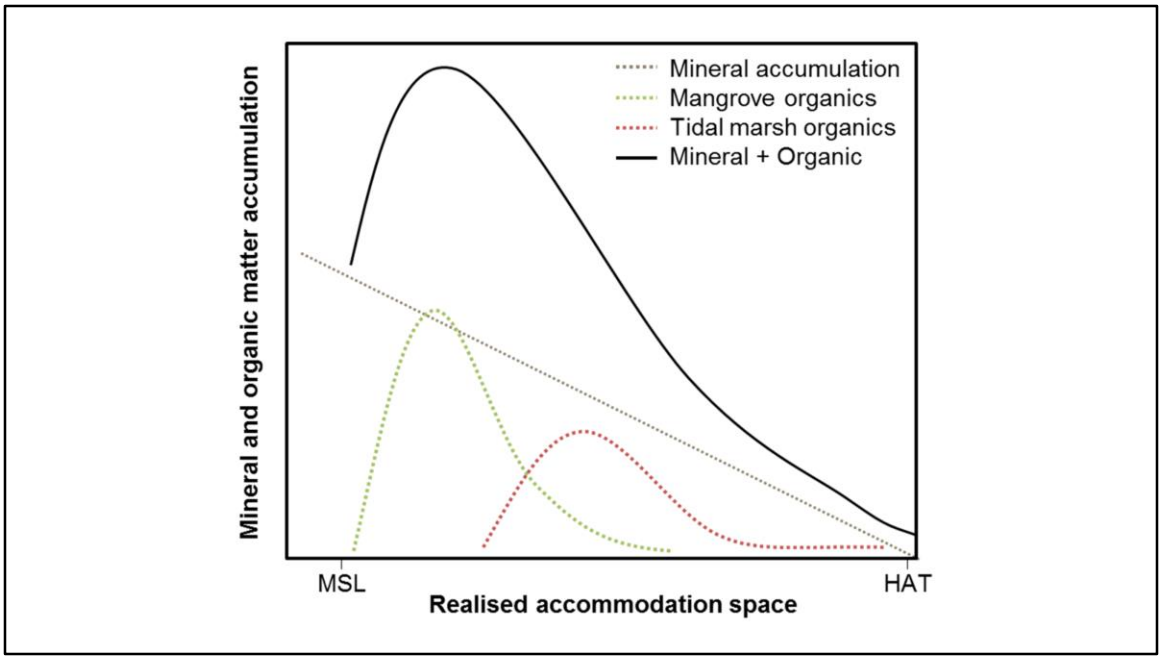

Fig. 3. Conceptual links between mineral and organic matter accumulation and realised accommodation space. Model of sediment characteristics with respect to realised accommodation space, here shown in two-dimensions to represent the three-dimensional wetland accommodation space. Sedimentation may vary between sites based on mineral and organic sediment availability, and the addition of root material, which is a function of the productivity of vegetation. For simplicity, and following others[30], mineral sediment addition was conceptualised to increase linearly with accommodation space, but may diminish with elevation in an exponential or polynomial manner. Accommodation space varies because of mineral and organic sediment accumulation, SLR and autocompaction.

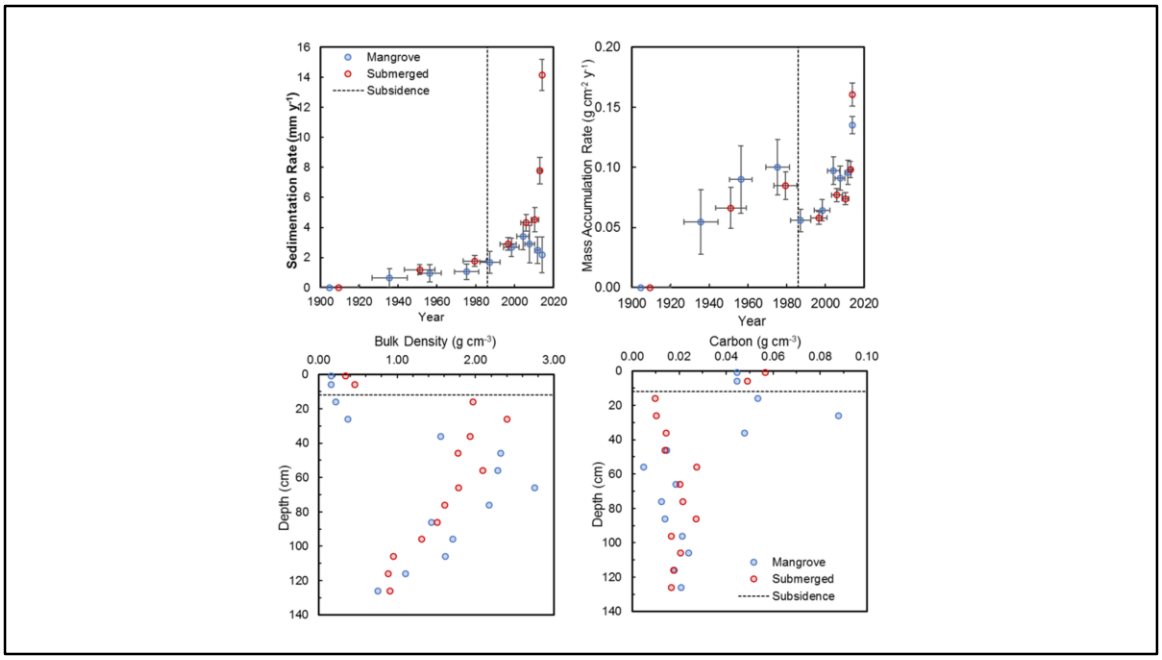

Fig. 4. Sediment accumulation and character related to available accommodation space. a) Calculated sedimentation rate (± standard error) and b) mass accumulation rate (± standard error) derived from ^{210}Pb dating; and c) bulk density and d) carbon density of mangrove (previously saltmarsh and terrestrial vegetation) and submerged (previously mangrove) sediments from Chain Valley Bay (outliers representing modern live root material at depth). The depth and associated age of sediments at which the subsidence event is evident indicated by dashed line. ^{210}Pb activity for mangrove and submerged cores and ^{137}Cs validation of ^{210}Pb chronology provided in Extended Data Fig. 2 and 3, respectively.

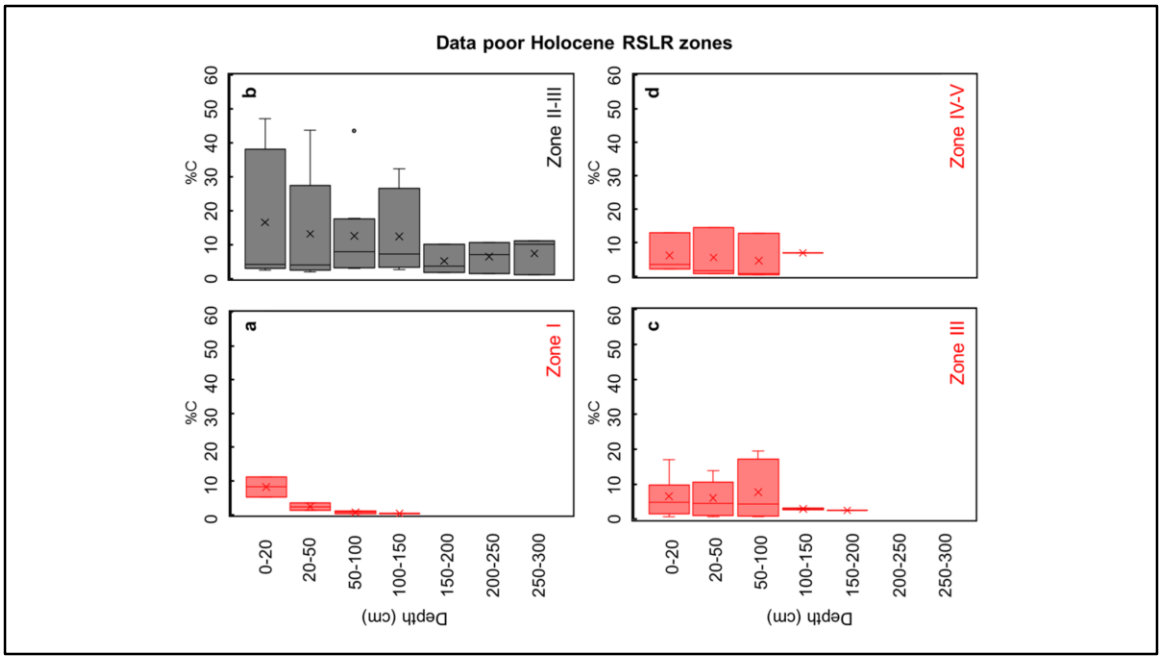

Extended Data Fig. 1 Relationship between late-Holocene RSLR and C concentration for data poor late Holocene RSLR zones and transitional zones. Boxplots of tidal marsh soil C concentration (%) for data poor Holocene relative sea-level rise (RSLR) zones and transitional regions: zone I (a), zone II-III transition (b), zone III (c), and zone IV-V transition (d).

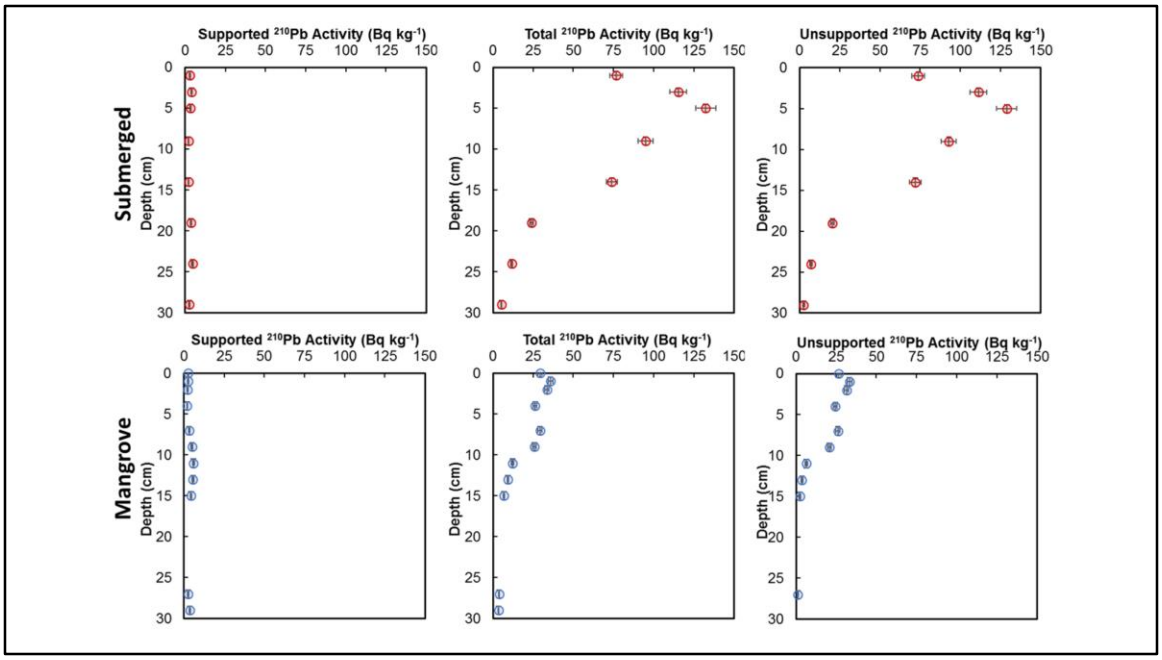

Extended Data Fig. 2 ^{210}Pb activity of submerged and mangrove sediments. Supported, total and unsupported ^{210}Pb activity (Bq/kg) for the submerged core sediments (a-c) and mangrove core sediments (d-f).

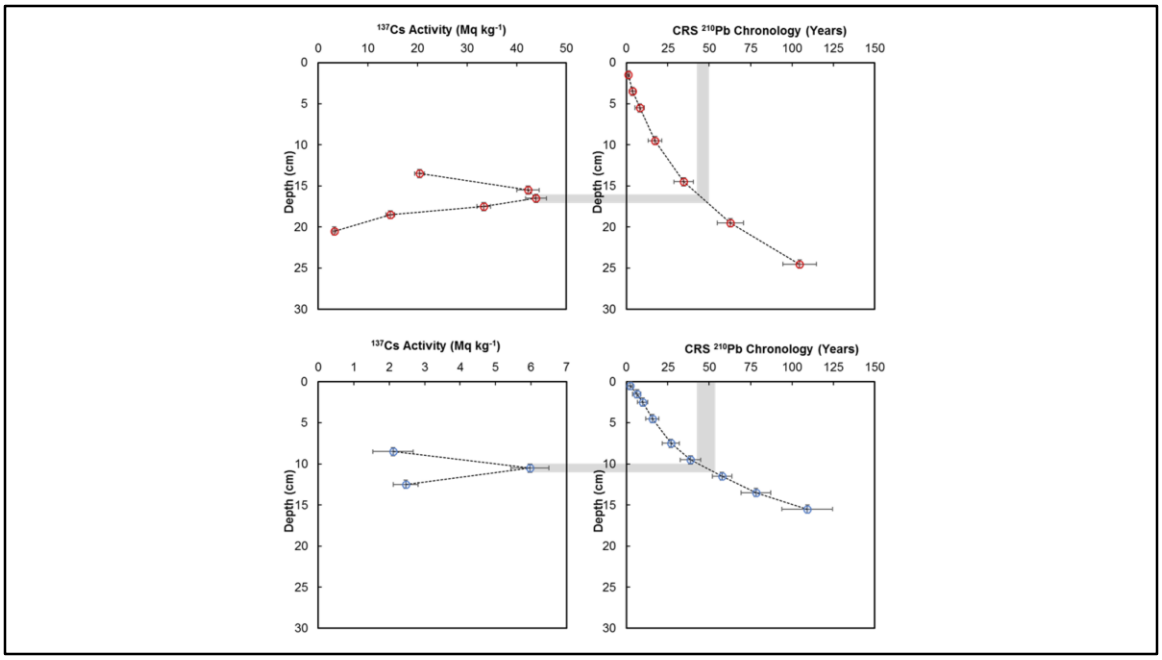

Extended Data Fig. 3 ^{137}Cs activity of submerged and mangrove sediments and ^{210}Pb chronology. ^{137}Cs activity (Bq/kg) and constant rate of supply (CRS) based ^{210}Pb chronology for submerged core sediments (a-b) and mangrove core sediments (c-d). The grey validation lines indicate that the ^{137}Cs activity peak, which approximates to 1964, corresponds to the CRS based ^{210}Pb chronology (NB: core dating occurred in 2014).

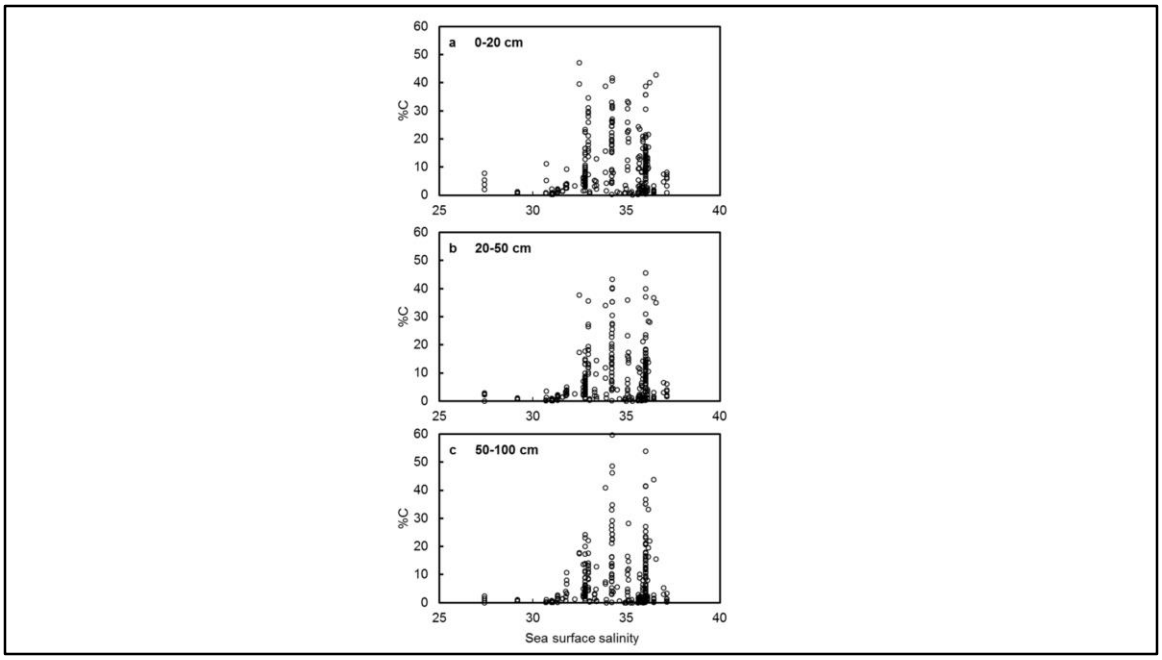

Extended Data Fig. 4 Relationship between sea surface salinity and C concentration over three depth intervals. Regression analysis of C concentration and global scale sea surface salinity, derived from the NASA Aquarius Satellite Mission, exhibited extremely weak relationships over the depth interval of a) 0-20 cm (R^2=0.07, P<0.001), b) 20-50 cm (R^2=0.07, P<0.01), and c) 50-100 cm (R^2=0.06, P<0.001).

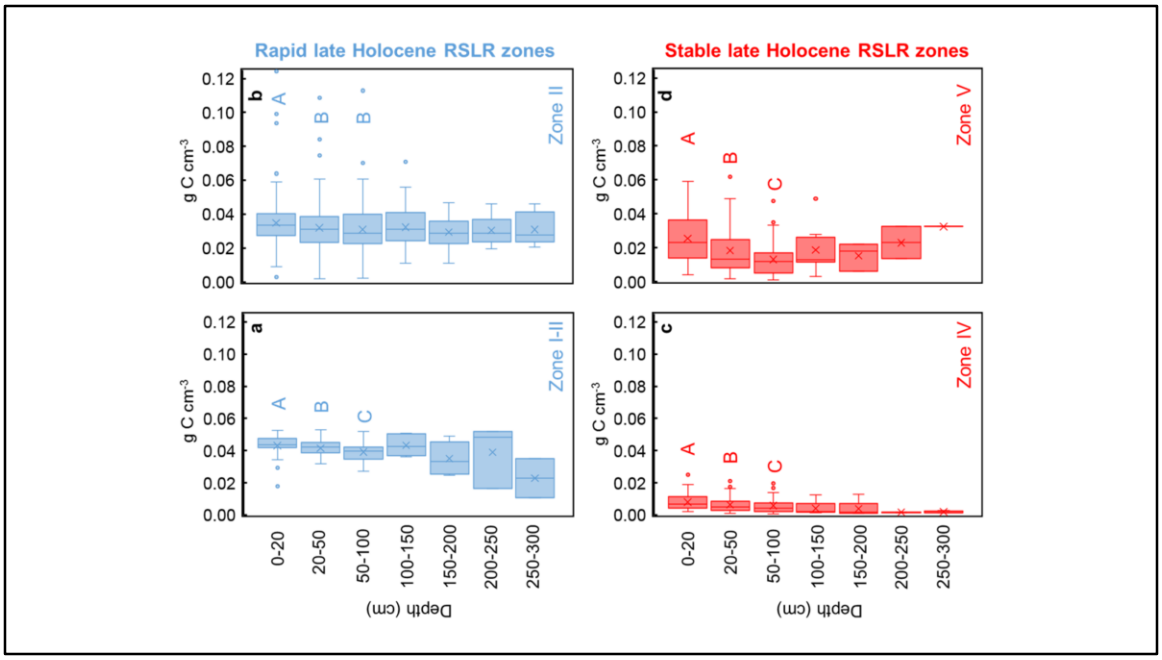

Extended Data Fig. 5 Relationship between late-Holocene RSLR and C density for data rich late Holocene RSLR zones and transitional zones. Boxplots of tidal marsh soil C density (g/cm^3) for data rich Holocene relative sea-level rise (RSLR) zones and transitional regions: zone I-II transition (a), zone II (b), zone IV (c), and zone V (d).